ITERATIVE SCATTER CORRECTION FOR DIGITAL TOMOSYNTHESIS USING COMPOSITION RATIO UPDATE AND GPU BASED MONTE CARLO SIMULATION

Kyung Sang Kim [a], Young Hoon Seong[b], Jongha Lee[b], Kwang Eun Jang[b] and Jong Chul Ye[a,]*

[a]Bio Imaging & Signal Processing Lab., Dept. of Bio& Brain Engineering, KAIST
291 Daehak-ro, Yuseong-gu, Daejon 305-701, Republic of Korea
[b] Samsung Advanced Institute of Technology, Samsung Electronics
14-1, Nong-seo dong, Kiheung-gu, Yongin, Kyunggi, Republic of Korea

ABSTRACT

In digital tomosynthesis (DTS), accurate scatter correction is often necessary for quantitative analysis. This is especially important because low energy x-ray of 10-40 keV, which is widely used for the breast imaging to enhance the contrast between adipose and glandular, results in high scatter fraction. In this paper, we propose an iterative scatter correction for digital tomopsynthesis using composition ratio update and GPU based Monte Carlo simulation (MCS). One of the technical difficulty in scatter estimation using MCS for tomosynthesis is that accurate segmentation of 3D volume is very difficult due to the low resolution of the reconstruction object. Thus, an intermediate surrogate object is introduced to represent composition ratio between adipose and glandular. We show that the composition ratio can be calculated using average attenuation coefficients. Another technical challenge is extremely high computational cost of MCS. We overcome this using GPU based ultra-fast MCS. Our results demonstrate that our iterative scatter correction using composition ratio update is indeed effective in improving the quality of the reconstruction object in a reasonable time frame.

Index Terms— Digital tomosynthesis, Monte Carlo simulation, Iterative scatter correction, composition ratio, GPU, CUDA

1. INTRODUCTION

Various imaging modalities such as CT, MRI and ultrasound have been widely used for breast imaging. Digital tomosynthesis (DTS) is the one of the promising new modalities for this purpose [1]. Compared to conventional CT, DTS has limited rotation angles, which results in low resolution images especially along axial direction. Moreover, due to the low energy x-ray of 10-40 keV, scatter fraction is higher. However, a hardware based scatter compensation method using an anti-scatter grid or a collimator is difficult to employ in DTS due to multiple x-ray incident angles. In this paper, we therefore propose a novel iterative scatter correction using composition ratio update and GPU based Monte Carlo simulation (MCS). Although the MCS based scatter correction has been developed for CT [2, 3], it is not widely used for digital tomosynthesis. This is because even though the reconstruction object should be accurately segmented for each material in MCS, accurate segmentation is difficult in DTS due to the low resolution reconstruction. Moreover, the MCS is computationally very expensive.

We overcome these technical difficulties using two techniques. First, rather than relying on the exactly segmented reconstruction, we introduce an intermediate surrogate reconstruction object representing the composition ratio between adipose and glandular. The ratio can be calculated by comparing the attenuation coefficients of the tomosynthesis reconstruction with the average attenuation coefficients of adipose and glandular. In addition, an iterative scatter correction that iterates MCS and the composition ratio update is shown to improve accuracy of the composition ratio estimation, hence the reconstruction quality as well. Second, to enable a practical MCS, we develop the ultra-fast MCS using GPU and CUDA.

Using numerical simulation and actual experiments with both homogeneous and inhomogeneous phantom, we demonstrate that the proposed method can effectively estimate the scatter contribution under 3 sec for each projection, and improves the final DTS reconstruction quality.

2. ITERATIVE SCATTER CORRECTION

2.1. Material composition model

Here, we assume that the breast tissue is mainly composed of two materials, adipose and glandular, since for most individuals the composition is characterized as a 70% adipose and 30% glandular mixture [4]. We then define the average attenuation coefficients of the adipose and glandular. The average attenuation coefficient ($\bar{\mu}$) for multi-spectrum x-ray can

This research was supported by Samsung Advanced Institute of Technology, Samsung Electronics (G01110128).

be calculated as follows [5]:

$$\bar{\mu} = \frac{\int \mu(E) \cdot I(E) dE}{\int I(E) dE} \quad , \tag{1}$$

where $\mu(E)$ denotes the attenuation coefficient of each material with energy E, and $I(E)$ is the intensity of the source energy spectrum. Using Eq. (1), the average attenuation coefficients for glandular and adipose material are first calculated. Since our model assume that every voxel is composed of only two materials, attenuation coefficient of voxel i is approximately linearly determined by the composition ratio between average attenuation coefficients of glandular and adipose as follows:

$$\mu_i \cong r_i \mu_g + (1 - r_i)\mu_a \quad , \tag{2}$$

where r_i denotes the composition ratio, and μ_i is the attenuation coefficient of voxel i of the reconstruction object, and μ_a and μ_g are the average attenuation coefficients of adipose and glandular, respectively. Our assumption is that even though we do not have exact composition of each voxel, the approximate composition ratio r_i in Eq. (2) is sufficient for scatter simulation. Recall that even though axial resolution of DTS is not good, the lateral resolution is sufficiently good. Since the lateral distribution of attenuation coefficient is a more dominant factor for the lateral distribution of scatter contributions on a detector, using DTS reconstruction we expect that the scatter estimate may become sufficiently accurate. Accordingly, we propose an iterative scatter correction algorithm which iterates the MCS and DTS reconstruction to improve accuracy of the composition ratio. After each iteration, the composition ratio $r_i = (\mu_i - \mu_a)/(\mu_g - \mu_a)$ is updated for each voxel using newly estimated μ_i value. Using the composition ratio value for each voxel, we can then perform another Monte Carlo simulation by calculating the photoelectric absorption, Rayleigh and Compton scattering properly for each material. After scatter correction, the DTS reconstruction is performed again after which the composition ratio is updated. This procedure iterates until the total composition ratio does not change. In the following, we will demonstrate the effectiveness of the iterative scatter correction and update of composition ratio.

2.2. Monte Carlo simulation

To perform the MCS, geometry parameters, x-ray source spectrum, attenuation and photoelectric absorption tables should be defined first. We used the source spectrum generator developed by Siewerdsen *et al* [6]. In our MCS, photon interactions such as photoelectric absorption, Rayleigh and Compton scattering are calculated.

A photon is generated from a source with random direction and random energy. An initial weight of the photon is determined as the magnitude in the spectrum corresponding to a chosen energy. Here, we assume that photon interactions do not occur in the air, and detector efficiency is 100%. Within an object, a photon travels, whose a path length is calculated by $l = -\ln(\xi)/\mu$, where μ is the attenuation coefficient defined by the energy and material, and ξ is a random number generated from the uniform distribution in the range [0,1]. Then, photoelectric absorption is calculated by the energy and material. Note that this is the step we need the composition ratio of the material. After migration, if the photon is in the object, scattering event occurs and the event is recorded by a scatter flag. To calculate scatter effect, we first define scattering angle θ. Here, $\cos\theta$ is assigned from an uniform random number in the range [-1,1]. We then calculate a differential cross section of Rayleigh and Compton scattering. Total differential cross section is then defined as follows:

$$\frac{d\sigma}{d\Omega} = \frac{d\sigma_R}{d\Omega} + \frac{d\sigma_C}{d\Omega}, \tag{3}$$

where

$$\frac{d\sigma_R}{d\Omega} = \frac{1}{2} r_e^2 (1 + \cos^2(\theta)) F^2(\chi), \tag{4}$$

$$\frac{d\sigma_C}{d\Omega} = \frac{1}{2} r_e^2 P_e^2 (P_e + P_e^{-1} - 1 + \cos^2(\theta)) S(\chi). \tag{5}$$

Here, σ_R and σ_C denote the cross section of Rayleigh and Compton scattering, respectively, r_e is the classical electron radius, and $P_e = \left(1 + (E/m_e c^2)(1 - \cos\theta)\right)^{-1}$ is the ratio of the scattered to incident photon energy E, and $F(\chi)$ and $S(\chi)$ denote the form factor and incoherent scattering function, χ is the transferred momentum expressed as

$$\chi = \frac{1}{\lambda} \sin(\frac{\theta}{2}) = \frac{E}{1.239} \sin(\frac{\theta}{2}) \quad , \tag{6}$$

where λ denotes the photon wavelength, and the unit of χ and E are nm^{-1} and keV, respectively. After calculating scatter, a directional vector is updated, and photon migration is calculated again. This procedure iterates until the photon is detected. After applying MCS, we can obtain the prompt and scatter projections by the scatter flag. Since prompt projection includes true and scatter events, we can calculate a scaling factor by comparing the simulated prompt with the measured data, and then scale the scatter distribution accordingly. This is one of the main advantages of MCS compared to tail fitting based scatter estimation, which is prone to error due to inaccuracy of scaling factor estimation. Finally, the scatter projection is subtracted from the original projection for scatter correction.

2.3. GPU implementation

We implemented MCS and maximum likelihood expectation maximization (MLEM) using GPU and CUDA. To maximally utilize the GPU, constant memory is used to store geometry parameters, attenuation and absorption tables to reduce variables in GPU kernels. In addition, texture memory is used

for the interpolation of a line integral [7]. By assigning a thread to a photon, it is difficult to maximally utilize the GPU due to the different number of scatter events for each photon. Thus, we only allow scatter up to three events. This improves performance by 25%. Since our MCS is designed for scatter correction, full resolution of detector is not necessary. Thus, we downsample the projection by increasing detector size to reduce the execution time. Execution time depends on the number of photons, and downsampling allows us to reduce the number of photons generated in GPU kernel. In this paper, we used 8 downsampling factor defined by considering the trade-off between the quality and the execution time.

3. EXPERIMENTAL RESULTS

To verify the proposed algorithm, we first performed a simulation experiment. A simulated phantom is composed of 5 targets of 1cm diameter spheres in a 50% glandular and 50% adipose mixture. The attenuation coefficients of targets are higher than glandular. Figs. 1 (a)-(d) show the ground truth, reconstructions using scatter uncorrected and corrected data after 2 iterations, respectively; and their cut views. In Fig. 1 (d), the scatter uncorrected object has lower attenuation coefficients and cupping artifact; however, the scatter corrected object is closer to the ground truth.

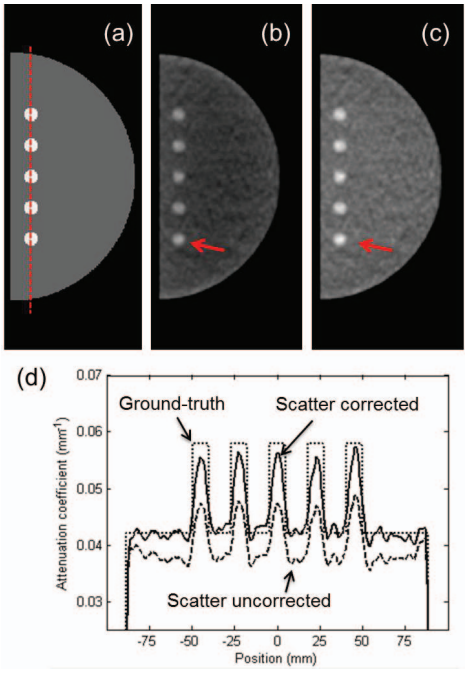

Fig. 1. (a) Ground truth of the numerical phantom; DTS reconstruction with (b) scatter uncorrected, (c) scatter corrected data using 2 iterations of proposed method, and (d) their cut views.

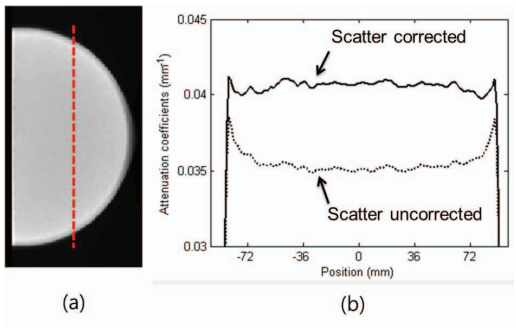

Fig. 2. Real phantom experiment of (a) a DTS reconstruction object, and (b) cut views of DTS reconstruction using scatter corrected and uncorrected projections.

Case	(a)	(b)	(c)	(d)
NMSE (%)	3.01	3.40	2.89	3.80
SPR (uncorrected)	0.093	0.130	0.104	0.119
SPR (corrected)	0.026	0.025	0.015	0.024

Table 1. NMSE and SPR results of the proposed method using (a) Al 1mm + 34 kVp, (b) Al 1mm + 38 kVp, (c) Al 1mm + Cu 0.03mm + 34 kVp and (d) Al 1mm + Cu 0.03mm + 38 kVp.

Next, we performed actual experiments using distinct source energy spectrums of 34, 38 kVp with Al and Cu filters, and homogeneous and inhomogeneous phantoms are used. Rotation range is -50° to 50° with 101 projections. We first validated our MCS based scatter correction by experiments using a homogeneous phantom composed of 50% adipose and 50% glandular with 5cm thickness. Figs. 2 (a) and (b) show the reconstruction object, and cut views of scatter uncorrected and corrected reconstructions, which shows that the cupping artifact is reduced significantly, and overall attenuation coefficients become higher after the correction. Table 1 compared the reconstruction results. Here, error was calculated by the normalized mean square error (NMSE) expressed as $e = ||O - P||_2^2/||O||_2^2$, where O and P denote the original and prompt projections, respectively, and we observed that the NMSE value can be less than 3%.

In addition, we compared the scatter to primary ratio (SPR). To calculate SPR in actual experiments, we assumed the primary value can be obtained from rim regions since they are less affected by scatter. The results show the SPR is 0.1$\sim$0.13 without scatter correction; however, SPR improves down to 0.02$\sim$0.03 after the scatter correction. Table 2 verified the effectiveness of iterative scatter correction and composition ratio update without knowing the composition ratio. Initial estimation of the total composition ratio of the scatter uncorrected object is nearly 0.1 corresponding to glandular of 10%. Thanks to the scatter correction, attenuation

Iteration	(a)	(b)	(c)	(d)
0	0.0947	0.0506	0.0960	0.1009
1	0.5344	0.5414	0.5566	0.5474
2	0.5126	0.4919	0.4860	0.4880
3	0.4802	0.5052	0.5080	0.5077

Table 2. Estimated composition ratio of the proposed reconstruction using homogeneous phantom with composition ratio of 0.5. The filter and kVp are set to (a) Al 1mm + 34 kVp, (b) Al 1mm + 38 kVp, (c) Al 1mm + Cu 0.03mm + 34 kVp and (d) Al 1mm + Cu 0.03mm + 38 kVp.

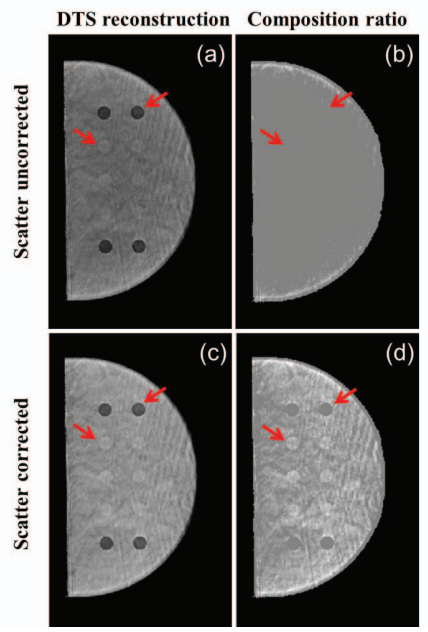

Fig. 3. DTS reconstruction results and corresponding composition ratio without scatter correction (a) (b), and after scatter correction (c) (d), respectively.

coefficients become more accurate, and the iterative scatter correction is effective in estimation of the composition object and improve the reconstruction. Table 2 shows the total composition ratio converges to almost 0.5 after 2 iterations for all filter and kVp combinations.

In addition, actual experiment using the inhomogeneous phantom was performed. Figs. 3 (a) and (c) are the scatter uncorrected and corrected reconstruction objects, and (b) and (d) are their estimated composition ratio. Here, Figs. 3 (c) and (d) are the results after 2 iterations. The composition ratio after 2 iterations shows the targets and patterns clearly, and the final reconstruction is much more improved compared to scatter uncorrected image.

In all the experiments, when we set the MCS quality of 3 % error, 80 millions of photons were required for a single projection, and the execution time takes under 3 sec per a single projection using Nvidia Tesla C2070, which is 73.4 times faster than CPU.

4. CONCLUSIONS

In this paper, we derived a fully iterative scatter correction algorithm using composition ratio update and GPU based Monte Carlo simulation. To calculate MCS, a composition ratio was necessary to represent the relative composition between adipose and glandular. For more accurate scatter correction by estimating composition ratio correctly, our proposed algorithm iterates MCS, DTS reconstruction and composition ratio update until the total composition ratio does not change. Even though we used approximate composition ratio due to the low resolution of DTS reconstruction rather than true reconstruction, our results demonstrated that the fully iterative scatter correction was effective in improving the resolution by reducing cupping artifact and scatter to primary ratio (SPR). Moreover, thanks to the GPU implementation, the execution time was under 3 sec for a single projection which is 73.4 times faster than CPU.

5. REFERENCES

[1] F. Diekmann, "Digital Breast Tomosynthesis and Breast CT," *Digital Mammography*, pp. 199–209, 2010.

[2] G. Poludniowski, PM Evans, VN Hansen, and S. Webb, "An efficient Monte Carlo-based algorithm for scatter correction in keV cone-beam CT," *Physics in Medicine and Biology*, vol. 54, pp. 3847–3864, 2009.

[3] W. Zbijewski and F.J. Beekman, "Efficient Monte Carlo based scatter artifact reduction in cone-beam micro-CT," *IEEE Transactions on Medical Imaging*, vol. 25, pp. 817–827, 2006.

[4] T.R. Nelson, L.I. Cerviño, J.M. Boone, and K.K. Lindfors, "Classification of breast computed tomography data," *Medical Physics*, vol. 35, pp. 1078–1086, 2008.

[5] S.C. Kappadath and C.C. Shaw, "Dual-energy digital mammography: Calibration and inverse-mapping techniques to estimate calcification thickness and glandular-tissue ratio," *Medical Physics*, vol. 30, pp. 1110–1117, 2003.

[6] JH Siewerdsen, AM Waese, DJ Moseley, S. Richard, and DA Jaffray, "Spektr: A computational tool for x-ray spectral analysis and imaging system optimization," *Medical Physics*, vol. 31, pp. 3057–3067, 2004.

[7] K. S. Kim and J. C. Ye, "Fully 3D iterative scatter-corrected OSEM for HRRT PET using a GPU," *Physics in Medicine and Biology*, vol. 56, pp. 4991–5009, 2011.